Research Article

Cyclophilin A binds to AKT1 and facilitates the tumorigenicity of Epstein-Barr virus by mediating the activation of AKT/mTOR/NF-κB positive feedback loop

Shuyu Xin [a,b,c,d,e], Lingzhi Liu [a,b,c,d,e], Yanling Li [a,b,c], Jing Yang [a,c], Lielian Zuo [a,c], Pengfei Cao [c,e], Qijia Yan [e], Shen Li [a,b,c], Li Yang [a,b,c], Taimei Cui [b], Jianhong Lu [a,b,c,d,e,*]

[a] Hunan Cancer Hospital/the Affiliated Cancer Hospital of Xiangya School of Medicine, Central South University, Changsha, 410013, China
[b] Department of Microbiology, School of Basic Medical Science, Central South University, Changsha, 410078, China
[c] The Key Laboratory of Carcinogenesis and Cancer Invasion of the Chinese Ministry of Education, NHC Key Laboratory of Carcinogenesis, Cancer Research Institute, Central South University, Changsha, 410078, China
[d] China-Africa Research Center of Infectious Diseases, Central South University, Changsha, 410013, China
[e] Department of Hematology, National Clinical Research Center for Geriatric Disorders, Department of Pathology, Xiangya Hospital, Central South University, Changsha, 410080, China

A R T I C L E   I N F O

A B S T R A C T

The AKT/mTOR and NF-κB signalings are crucial pathways activated in cancers including nasopharyngeal carcinoma (NPC), which is prevalent in southern China and closely related to Epstein-Barr virus (EBV) infection. How these master pathways are persistently activated in EBV-associated NPC remains to be investigated. Here we demonstrated that EBV-encoded latent membrane protein 1 (LMP1) promoted cyclophilin A (CYPA) expression through the activation of NF-κB. The depletion of CYPA suppressed cell proliferation and facilitated apoptosis. CYPA was able to bind to AKT1, thus activating AKT/mTOR/NF-κB signaling cascade. Moreover, the use of mTOR inhibitor, rapamycin, subverted the activation of the positive feedback loop, NF-κB/CYPA/AKT/mTOR. It is reasonable that LMP1 expression derived from initial viral infection is enough to assure the constant potentiation of AKT/mTOR and NF-κB signalings. This may partly explain the fact that EBV serves as a tumor-promoting factor with minimal expression of the viral oncoprotein LMP1 in malignancies. Our findings provide new insight into the understanding of causative role of EBV in tumorigenicity during latent infection.

1. Introduction

Epstein-Barr virus (EBV) is an important causative agent in several malignancies such as Burkitt's lymphoma and nasopharyngeal carcinoma (NPC) (Bruce et al., 2015; Huang et al., 2018; Lo et al., 2012). NPC is a unique epithelial neoplasm that derives from the pharyngeal mucosal epithelium, which occurs prevalently in southern China and Southeast Asia (Bruce et al., 2015). About 90% of NPC in endemic areas could be detectable with EBV genome. There are two different NPC subtypes, including differentiated and undifferentiated NPC. Undifferentiated NPC with highly invasive and metastatic characters occupies the most portion of suffering population (Lin et al., 2014; Nakanishi et al., 2017). In recent years, with the advancement of diagnostic technologies and combinative use of radiotherapy and chemotherapy, the overall prognosis of NPC has been promoted

greatly (Nakanishi et al., 2017). However, distant metastasis remains an intricate issue. Since we have entered an era of precision medicine, more molecular biomarkers should be explored in the diagnosis and treatment of NPC.

In order to evade host surveillance, EBV infects host cells and establishes lifelong latent infections (Liu et al., 2017). During the latent infection, EBV expresses limited genes which contribute to the development of malignances. Among these EBV-encoded proteins, the oncoprotein of latent membrane protein 1 (LMP1) plays an essential role in the transformation of B cells, mediating various pathways such as NF-κB signaling (Bentz et al., 2012; Kang and Kieff, 2015; Shair et al., 2018). However, the mechanism of LMP1 involved in EBV pathogenesis in NPC remains to be fully clarified. NF-κB signaling has been certified as a significant pathway in the tumorigenesis of NPC (Chung et al., 2013; Takada et al., 2017; Tu et al., 2018; Yi et al., 2018).

AKT/mTOR is another critical intracellular signaling pathway involved in a variety of physiological and pathological processes, including cell proliferation, survival and invasion (Carnero et al., 2008; Shih et al., 2017). As it is demonstrated, aberrant activation of AKT/mTOR is usually encountered in cancer development (Baek et al., 2017; Kim et al., 2013; Mohan et al., 2016; Polivka and Janku, 2014; Siveen et al., 2014). AKT, also known as protein kinase B (PKB), is the central node of this pathway. Activated AKT can act downstream of PI3K to regulate cellular processes (Manning and Cantley, 2007; Manning and Toker, 2017). mTOR (mammalian target of rapamycin) is also a major protein in this pathway that is able to act upstream or downstream of AKT (Yu and Cui, 2016). AKT/mTOR has been reported as an active pathway in NPC (Liu et al., 2019b). And, EBV encoded LMP1 is able to activate this pathway with the mechanism unclear. Since AKT/mTOR pathway is involved in important cellular processes, targeting the activation of this pathway can be expected to have an impact on therapeutic strategies against cancer.

Cyclophilin A (CYPA), which is encoded by *PPIA* gene, is a crucial member of immunophilin family that involved in the vast of activities (Dawar et al., 2017). CYPA plays important roles in a number of cancers, such as melanoma and hepatocellular carcinoma (Guo et al., 2016; Wang et al., 2017; Yuan et al., 2016; Zhu et al., 2015). In our previous studies, the expression of CYPA was found to be upregulated in NPC tissues from the early stage of NPC development (Yang et al., 2014). CYPA expression in sera exosomes was also increased in NPC patients, showing as a potential diagnosis biomarker in NPC. We also found that the expression of exosomal CYPA is positively correlated with that of exosomal LMP1 in NPC sera (Liu et al., 2019a). However, the mechanism and role of CYPA overexpression in EBV-associated NPC remain to be explored. In the present study, CYPA expression was confirmed to be upregulated by EBV-encoded LMP1 through the activation of NF-κB. CYPA was able to proliferate cell growth and inhibit apoptosis of NPC cells. Furthermore, CYPA is a new binding protein of AKT1, thus activating the AKT/mTOR/NF-κB signaling pathway. Actually, with the mediation of CYPA, EBV-LMP1 potentiates a positive feedback loop, NF-κB/CYPA/AKT/mTOR/NF-κB, which ensures a constant role in the tumorigenicity. The results may help us to understand the viral etiological role in NPC development, providing potential biomarkers for the therapeutics of EBV-associated NPC.

2. Materials and methods

2.1. Cell lines

All cell lines are kept regularly in our laboratory. C666-1 is an EBV-positive NPC cell line (Cheung et al., 1999), while HONE1, CNE1 and HK1 are EBV-negative NPC cell lines (Zuo et al., 2019). All the NPC cell lines were cultured in RPMI-1640 medium supplemented with 10% fetal calf serum (Gibco, Grand Island, NY, USA) at 37 °C in the atmosphere with 5% CO_2. The C2089 cell line is an EBV-positive cell line with the whole EBV genome stably infected human embryonic kidney 293 cells (Delecluse et al., 1998; Zuo et al., 2015). The 293-LMP1 cell line was previously established that stably expressed EBV-LMP1 (Zuo et al., 2019). The 293T is preserved in our laboratory (Xin et al., 2019). All the cell lines derived from 293 were grown in Dulbecco's modified Eagle's medium (DMEM) supplemented with 10% fetal calf serum (Gibco).

2.2. Plasmids and siRNA

The overexpression plasmids of pCAGGS-AKT1-HA (AKT1-HA) was constructed by using the pCAGGS vector, which was a gift from Dr. Harty (Lu et al., 2013, 2014). Flag-tagged LMP1 was cloned into the pcDNA3.1 vector (LMP1-Flag). We previously constructed a CYPA expression plasmid pCAGGS-Flag-CYPA (Flag-CYPA) (Xin et al., 2019). The pCMV3-p65 overexpression plasmid was a product of the Sino Biological Inc. (HG12054-NF, Beijing, China). CYPA-specific siRNA and its negative control that used for cell transfection were synthesized by Ruibo

Company (Guangzhou, China) as described previously (Xin et al., 2019). Cell transfection was performed onto 60% confluent cells using Lipofectamine 3000 (Invitrogen; Thermo Fisher Scientific, Inc. Carlsbad, CA, USA) according to the manufacturer's protocol.

2.3. CRISPR/cas 9 technique for CYPA knockout

An oligo of gRNA that targets the N-terminus of *CYPA* gene was obtained from Ruibo Biological Inc. (Guangzhou, China) and cloned into lentiCRISPRv2 plasmid. The resulted plasmid, lentiCRISPRv2-CYPA, along with the psPAX2 packaging plasmid and Pmd2.G envelope plasmids were co-transfected into 293T cell line to harvest the lentivirus supernatant. Then, the lentivirus supernatant was co-cultured with 293 cell line, and after 48 h post-transfection, puromycin (1 μg/mL) was added into culture medium for screening and establishment of stable CYPA knockout 293 cell line (293 KOCYPA). The CYPA sgRNA sequences are as following: sgRNA-L: CACCGTGCCAGGACCCGTATGCTTT, sgRNA-R: AAACAAAGCATACGGGTCCTGGCAC. Sequencing results of *CYPA* gene in 293 KOCYPA cell line was shown in Supplementary Fig. S1.

2.4. Western blotting

Western blotting (WB) analysis was performed regularly (Lu et al., 2010). Briefly, cells were lysed with RIPA buffer (Beyotime Biotechnology, Shanghai, China) containing a protease inhibitor phenylmethanesulfonyl fluoride (PMSF, Dingguo, Beijing, China) and phosphatase inhibitor (MCE, American) to obtain total proteins. Equivalent amounts of denatured proteins were resolved by sodium dodecyl sulfate-polyacrylamide gel electrophoresis using a 10% gel and transferred onto a polyvinylidene difluoride membrane (Millipore, Billerica, MA, USA). The membrane was blocked for 60 min with 5% non-fat milk at room temperature and was incubated with a primary antibody overnight at 4 °C. Then, the membrane was incubated with corresponding secondary antibody at 37 °C for an hour. Finally, the PVDF membrane was covered with Immobilon western chemiluminescent HRP substrate (cas. no WBKLS0100, Millipore) and developed in Bio-Rad Gel Doc XR + system (Bio-Rad, Hercules, CA, USA).

The specific antibodies in this approach were: the LMP1 mouse mAb (DAKO Lifetech, Glostrup, Denmark, M0897), p-NF-κB (p65) rabbit mAb (CST, Chicago, USA, #3033), NF-κB rabbit mAb (Millipore, 06-418), CYPA rabbit mAb (Proteintech, Chicago, USA), AKT1 rabbit mAb (CST, #2938S), AKT1 mouse mAb (Beyotime, Shanghai, China, AF0045), p-AKT1 (Ser473) Rabbit mAb (CST, #9018S), p-mTOR (Ser2448) Rabbit mAb (ABclone, Wuhan, China, AP0115), mTOR rabbit mAb (SAB, California, USA, 41187), p-p70S6K (Thr389) Mouse mAb (CST, #9206S), p70S6K Rabbit mAb (CST, #2708S), GAPDH Rabbit pAb (Proteintech, 10494-I-AP). HRP goat anti-mouse IgG (ABclone, AS003) and HRP goat anti-rabbit IgG (ABclone, AS014) were used as secondary antibodies.

2.5. Cell viability assay

Cell viability was tested by using a Cell Counting Kit-8 (CCK-8; Dojindo Molecular Technologies, Inc., Kumamoto, Japan) following the manufacturer's protocol. Cells were transfected with siRNA-CYPA and the corresponding siRNA-NC. Then, after an appropriate period of incubation, the optical density was measured at the time of 24 h, 48 h, 72 h and 96 h with a wavelength of 450 nm. Based on the calculated number of viable cells, the growth curve was obtained.

2.6. Cell apoptosis detection

After 48 h post-transfection, cells were washed twice and obtained. Then, cell apoptosis analysis was performed using flow cytometry with AnnexinV-FITC and propidium iodide (PI) staining (Dojindo Molecular Technologies) following the manufacturer's instructions. Events were recorded from samples using a CytekTM Aurora Flow Cytometer (Cytek

Biosciences, USA) and analyzed using FlowJo v10 software (Verity Software House, Topsham, ME).

Tunel assay was used for the apoptosis detection in tissues. A commercial situ apoptosis detection kit (Roche Diagnostics, Germany) was used according to the manufacturer's protocol. The images were obtained by a conventional microscope.

2.7. Co-immunoprecipitation assay (co-IP)

For the co-IP assay, pCAGGS-AKT1-HA and pCAGGS-Flag-CYPA were transfected into 293 cells with TurboFect™ Transfection Reagent (R0534, Thermo Scientific). Then the cells were collected and lysed at 48 h post-transfection. The resulting cell lysates were incubated with 1–2 μg of the corresponding antibody for IP overnight at 4 °C, followed by incubation with 20 μL of Protein A/G agarose beads (Bimake, Selleck, American) for 2 h at room temperature. The protein A + G agarose beads were washed for three times with lysis buffer and resuspended in 30 μL 2 × sodium dodecyl sulfate-polyacrylamide gel electrophoresis (SDS-PAGE) loading buffer. These samples were boiled for 10 min and then subjected to WB analysis.

2.8. Immunofluoresence (IF) assay

The procedure of IF assay was carried out as previously described (Xin et al., 2019). In brief, 293T cells were seeded on glass slides in six-well plates, fixed in 4% formaldehyde, permeabilized with 0.5% Triton X-100, and then blocked with fresh 10% normal goat serum for 1 h. The cells were incubated with primary antibodies at 4 °C overnight. The secondary antibodies were incubated for 1 h at 37 °C. Subsequently, the cells were washed with PBS and applied with Hoechst 33342. Images were acquired with a florescent microscope (Olympus, Tokyo, Japan).

2.9. Nude mice experiment

Male BALB/c nude mice of 4-week-old were obtained from Hunan SLAC Laboratory Animal CO. LTD and housed in the Laboratory Animal Center of Central South University (Changsha, China). Nude mice were maintained at 22–25 °C with 50–60% humidity, with free access to food and water in a specific pathogen-free laboratory animal facility. Stably 293 KOCYPA cells and 293 cells (2×10^6) were subcutaneously injected into the axillary flank of three nude mice for each group. At 45 days post-injection, the nude mice were sacrificed, and the tumors were used for further experiments. The research was approved by the Ethics Committees of Central South University, Hunan, China.

2.10. Immunohistochemistry (IHC)

Expressions of CYPA and Ki-67 in the xenografted tumors were confirmed by IHC analysis, which was conducted as described previously (Zuo et al., 2019). In brief, tumor specimens were formalin-fixed, paraffin-embedded, and sectioned conventionally. A manufactured kit (Boster Inc.) was used for further detection according to the manufacturer's protocol. Anti-CYPA rabbit monoclonal antibody was obtained from Proteintech (Proteintech). The slides were observed under a microscope.

2.11. Protein-protein interaction prediction

STRING was used for predicting the possible protein-protein interaction (https://stringdb.org/cgi/input.pl?sessionId=9AurP7Mb1YTo&input_page_show_search=on).

2.12. Statistical analysis

Statistical analyses were performed using GraphPad Prism 5 (GraphPad Software Inc., La Jolla, CA, USA) and Flowjo 10 (Verity
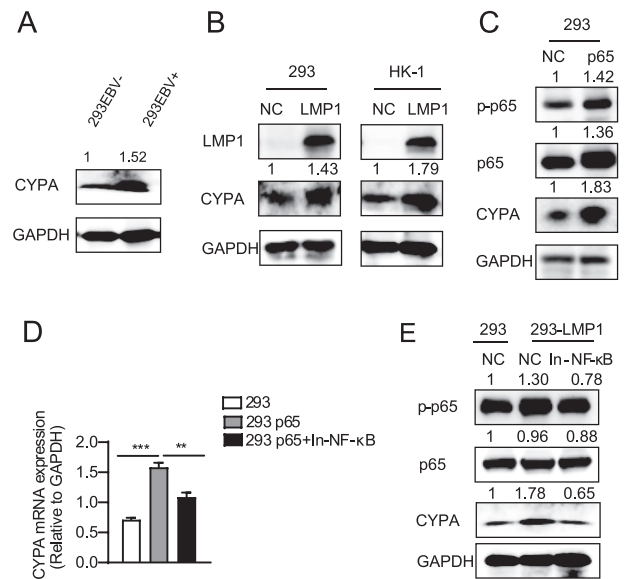

Fig. 1. EBV-encoded LMP1 promotes CYPA expression via NF-κB activation. **A** The detection of CYPA protein in EBV-negative and positive 293 cells by Western blot assay. **B** The expression of CYPA in 293-LMP1 (stably expressed with LMP1) cells and EBV-negative HK-1 cells. **C** The effect of NF-κB (p65) overexpression on CYPA expression in 293 cells. For normal control (NC), corresponding empty vector (pCMV) was used (2 μg/well for each plasmid). **D** The effects of NF-κB activation and inhibition on CYPA mRNA levels evaluated by RT-qPCR in 293 cells. **E** The effect of NF-κB inhibitor (In-NF-κB) on the expression of p-p65 and CYPA in 293-LMP1 cells. For the NF-κB inhibitor in **D** and **E**, the cells were cultured in medium containing 4 μmol/L of inhibitor. At 24 h or 36 h post-treatment, the cell proteins and total RNA were extracted, respectively. Data were shown as mean ± standard error of mean of at least three independent experiments. Statistical analysis was performed by Student's *t*-test. **$P < 0.01$, ***$P < 0.001$.

Software House, Topsham, ME). Data are presented as mean ± standard error of measurement (SEM). Comparisons between two groups were performed using Student's *t*-test. $P < 0.05$ was considered statistically significant.

3. Results

3.1. EBV-encoded LMP1 promotes CYPA expression via NF-κB activation

Since the expression of sera exosomal CYPA and EBV-LMP1 was previously found to be positively correlated (Liu et al., 2019a), we tried to explore whether EBV-LMP1 regulated CYPA expression in cells. The results showed that the expression of CYPA was increased in EBV-positive cells and in cells with LMP1 overexpression (Fig. 1A and B). To further confirm whether NF-κB, which is the major signaling activated by LMP1 (Zuo et al., 2015), regulated CYPA expression, the pCMV-NF-κB (p65) plasmid was transfected into 293 cells. As it shown in Fig. 1C, the expression of CYPA was increased after overexpression of p65, whereas the treatment of NF-κB inhibitor reduced the CYPA expression in 293-LMP1 cell line (Fig. 1E). The expression of CYPA mRNA levels was also increased by p65 and inhibited by NF-κB inhibitor (Fig. 1D). The results demonstrated that LMP1 promotes CYPA expression via NF-κB activation.

3.2. CYPA facilitates cell proliferation and inhibits apoptosis

We detected the impact of CYPA on the cell proliferation and apoptosis, which are the fundamental cellular biological functions in tumorigenicity identification. When CYPA was knocked down using siRNA in NPC cell lines, the cell proliferation was attenuated significantly
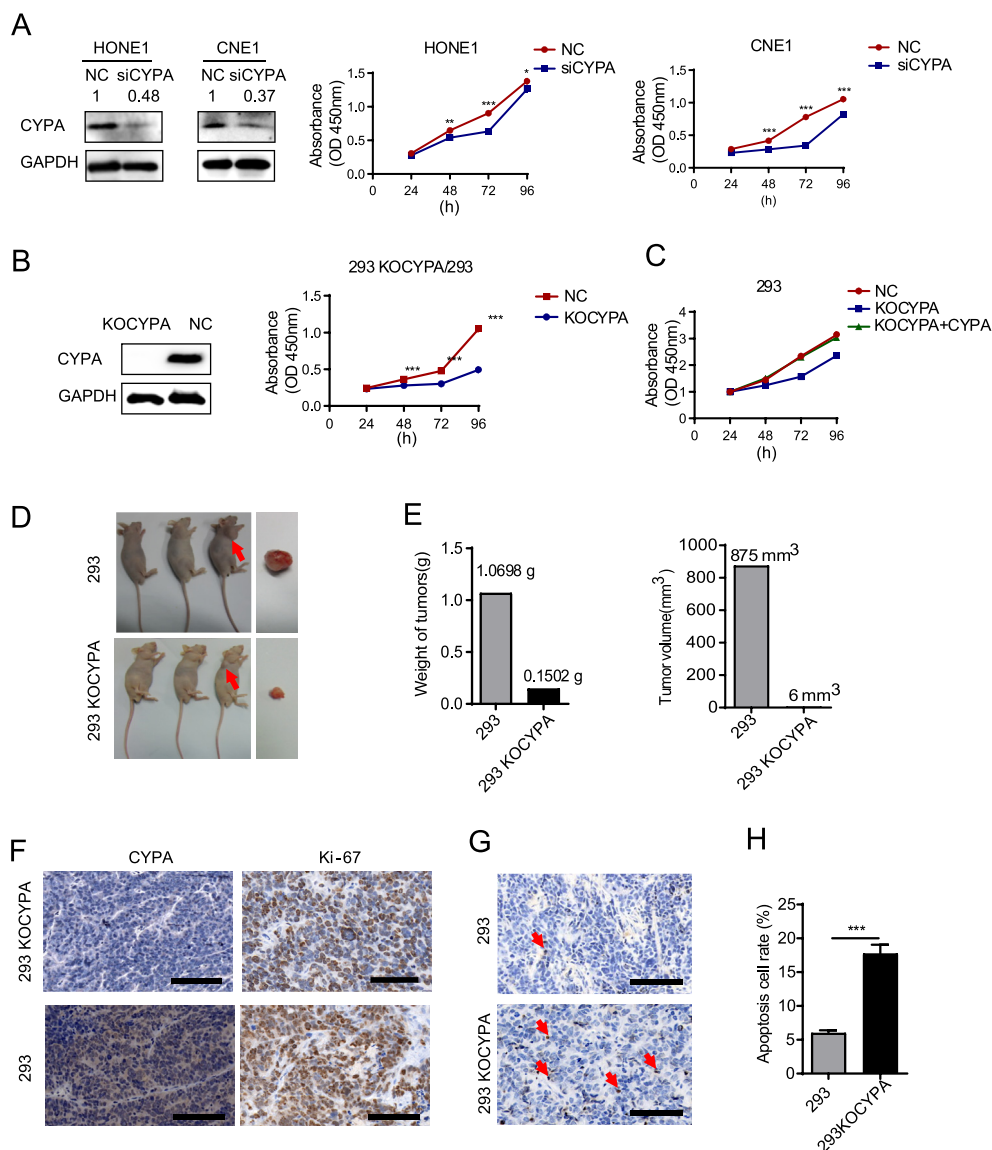
Fig. 2. The effect of CYPA on cell proliferation and xenografted tumor apoptosis. **A** The effect of CYPA knockdown by using siRNA on cell proliferation in naso-pharyngeal carcinoma cell lines, HONE1 and CNE1. At 48 h post-transfection with siRNA, the cells were collected and Western blot assay was performed for the analysis of CYPA protein level. CCK8 assay was performed to evaluate the cell viability at indicated time point. **B** CYPA knockout (KOCYPA) 293 cell line was constructed through CRISPR/Cas9 technique. CCK8 assay was performed to evaluate the cell viability at indicated time point. **C** The effect of CYPA overexpression in 293 KOCYPA on cell proliferation. The Flag-CYPA plasmid (2 μg/well) were transfected into 293 KOCYPA cells, at the indicated time point post-transfection, the cells were collected and cell viability was detected by CCK8 assay. **D** The effect of CYPA knockout on the growth of xenografted tumor in nude mice. The 293 KOCYPA cells or 293 cells (2×10^6, 100 μL) were subcutaneously injected into the axillary flank of nude mice, respectively (n = 3). At 45 days post-inoculation, the nude mice were sacrificed and photographed, and the tumors were then taken out and photographed. Red arrows indicate the grown tumors in mice. **E** Weight and volume of xenografted tumors. **F** IHC was performed to detect the CYPA and Ki-67 in xenograft sections. Scale bar, 100 μm. **G** Tunel staining of xenograft tumor sections. Red arrows indicate positively staining. Scale bar, 100 μm. **H** The quantitative result of **G**. Data were shown as mean ± standard error of mean of three independent experiments. Statistical analysis was performed by Student's t-test. *$P < 0.05$, **$P < 0.01$, ***$P < 0.001$.

by cell viability assay. And CYPA protein expression was evaluated by WB assay (Fig. 2A). Inhibited cell proliferation was also observed in 293 KOCYPA cells (Fig. 2B), whereas the ectopic expression of CYPA in 293 KOCYPA restored the cell proliferation (Fig. 2C). Furthermore, the experiment in nude mice model showed that 293 KOCYPA formed a smaller xenografted tumor and diminished tumor growth than the control group (Fig. 2D and E). IHC staining of the tumor sections for the expression of CYPA and the nuclear proliferating antigen Ki-67 displayed that 293 KOCYPA group had weaker proliferation ability than the 293 control (Fig. 2F). Tunel assay on the tumor sections showed increased

apoptosis for 293 KOCYPA group compared with the control group (Fig. 2G and H).

Annexin V-FITC examination and flow cytometry technique were employed for the apoptosis analysis of NPC and 293 cell lines with CYPA knockdown or knockout. The result showed that apoptosis was induced in siCYPA NPC cells, HONE1 and CNE1 (Fig. 3A). The result was similar in 293 KOCYPA cells, and CYPA ectopic expression in 293 KOCYPA restored the inhibition of apoptosis (Fig. 3B).

These results implied that upregulated CYPA might oppositely increase the tumorigenesis in these cell types.
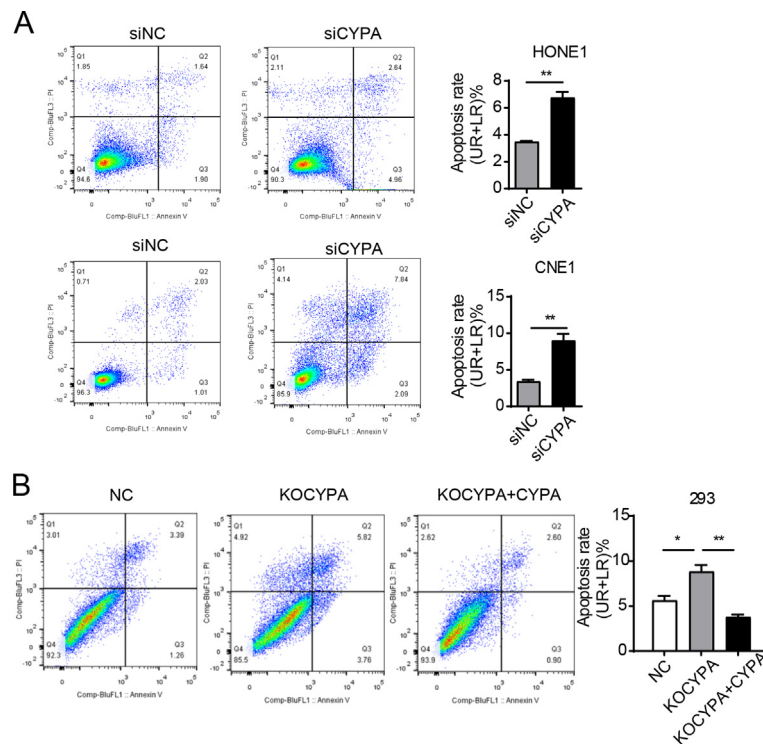
Fig. 3. The effect of CYPA depletion or restoration on cell apoptosis evaluated by flow cytometry (FCM) assay. **A** After transfected with siRNA targeting CYPA, HONE1 and CNE1 cells were collected and stained with Annexin V & PI. Cell apoptosis was evaluated by FCM. Apoptosis rate was calculated. UR, upper right, representing late apoptotic cells; LR, lower right, representing early apoptotic cells. **B** Effect of CYPA knockout and CYPA ectopic expression on cell apoptosis. For the CYPA over-expression, the 293 KOCYPA cells were transfected with Flag-CYPA plasmid (2 μg/well in 6-well plate). At 24 h post-transfection, the cells were collected and used for FCM assay. Data were shown as mean ± standard error of mean of three independent experiments. Statistical analysis was performed by Student's *t*-test. *$P < 0.05$, **$P < 0.01$.

3.3. CYPA binds to AKT1

The STRING online software was firstly used to predict that CYPA (*PPIA*) potentially interacted with AKT (AKT1) (Fig. 4A). To confirm the interaction between CYPA and AKT1, endogenous and exogenous co-IP experiments were carried out in 293 and HK-1 cells separately. As the result shown in Fig. 4B–D, CYPA-AKT1 binding was validated. In order to investigate the ability of LMP1 to influence the CYPA-AKT1 binding, a co-IP assay was performed following ectopic expression of LMP1 and AKT1 by using AKT1-HA for the pull-down and endogenous CYPA was detected. As shown in Fig. 4E, LMP1 strengthened the CYPA-AKT1 interaction. Additionally, the IF assay also displayed the increased CYPA expression and suggested the enhanced co-localization of CYPA-AKT1 in the presence of LMP1 (Fig. 4F). The expression of LMP1 detected by RT-qPCR is shown in Supplementary Fig. S2.

3.4. CYPA is required for the activation of AKT/mTOR/NF-κB signaling cascade

Since CYPA binds to AKT1, which is able to mediate the activation of mTOR/NF-κB signaling cascade, we further detect the influence of CYPA on the AKT/mTOR/NF-κB pathway. The p70 ribosomal protein S6 kinase (p70S6K) is a downstream target of mTOR (Bahrami et al., 2014; Manning and Toker, 2017). The results exhibited that the knockdown by siCYPA reduced the expression of p-AKT1, p-mTOR, p-p70S6K, and p-NF-κB (p-p65) in NPC cells (Fig. 5A). CYPA knockout also blocked AKT activation (Fig. 5B), while the ectopic expression of CYPA in 293 KOCYPA cells rescued the expression of p-AKT1, p-mTOR, p-p70S6K, and p-NF-κB (Fig. 5C). The results reveal that CYPA is

required for the activation of AKT/mTOR/NF-κB signaling cascade in NPC and 293 cells.

3.5. Rapamycin subverts the NF-κB/CYPA/AKT/mTOR/NF-κB positive feedback loop

Since CYPA is also upregulated by NF-κB (Fig. 1) and activated NF-κB via AKT/mTOR simultaneously, a positive feedback loop of NF-κB/ CYPA/AKT/mTOR/NF-κB should be formed. In order to further confirm this loop and whether the loop could be restrained, we used the mTOR inhibitor, rapamycin, to treat EBV-positive C666-1 and C2089 cells. As shown in Fig. 6, the expression of p-AKT1, p-mTOR, p-p70S6K, p-NF-κB, and CYPA were repressed in all these cell lines after treatment of rapamycin. Therefore, the results demonstrate that rapamycin subverts the NF-κB/CYPA/AKT/mTOR/NF-κB positive feedback loop.

4. Discussion

The EBV is the first confirmed human tumor virus, which is involved in the oncogenesis of NPC and several other malignancies (Gandhi et al., 2004; Nishikawa et al., 2018; West, 2014; Wu et al., 2018). Whereas, the mechanism of this unique virus in NPC have not been fully illustrated. CYPA has been found to be overexpressed and involved in the development of several cancers such as colorectal cancer and breast cancer (Chu et al., 2021; Davra et al., 2020; Yamamoto et al., 2020), and is regarded as a key player of human diseases (Nigro et al., 2013). In the previous work of our laboratory, CYPA was found to be upregulated in both NPC tissues and sera exosomes (Liu et al., 2019a; Yang et al., 2014). The overexpression of CYPA was also found to promote the replication and
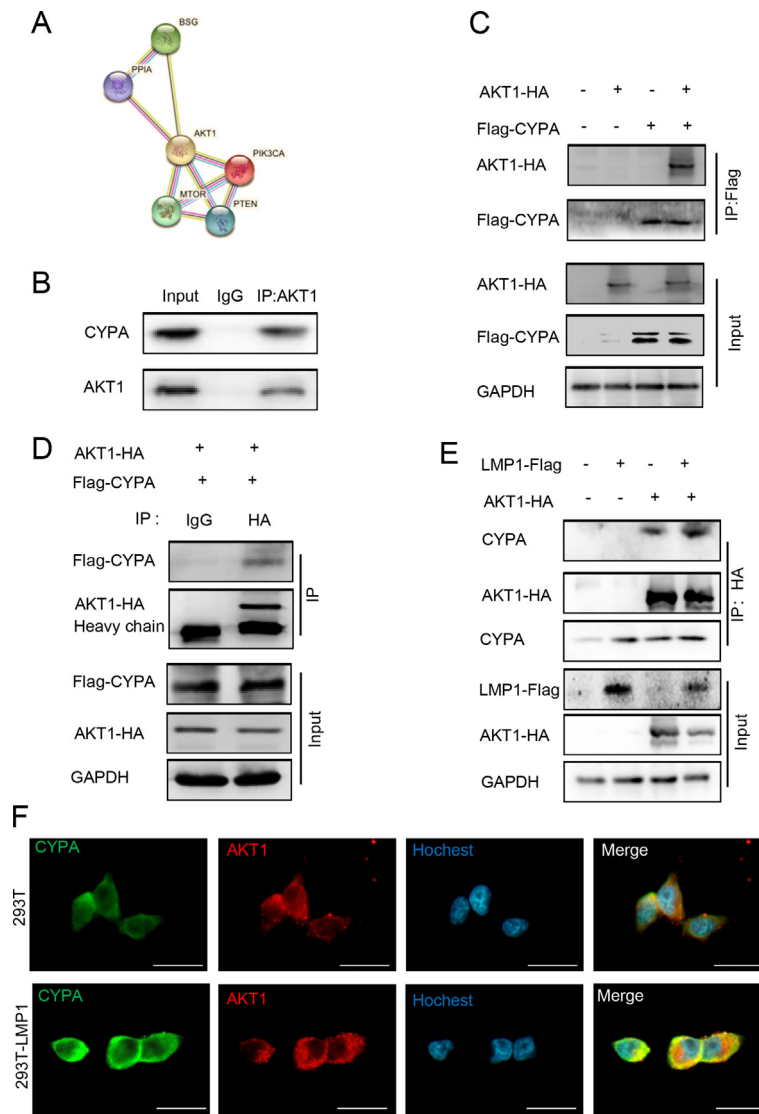
Fig. 4. The interaction of CYPA and AKT1. **A** STRING online software predicts the potential interaction between CYPA and AKT1. **B** Endogenous CYPA interacts with AKT1 in nasopharyngeal carcinoma HK-1 cells that detected by co-IP. The anti-AKT1 antibody was used for pull-down, and CYPA was detected by Western blot (WB). **C** Exogenous CYPA interacts with AKT1. The 293 cells were transiently transfected with Flag-CYPA and/or AKT1-HA plasmids (4 μg/well of each plasmid in 100 mm dish). At 48 h post-transfection, the cells were collected and subjected to co-IP assay. The anti-Flag antibody was used for pull-down, and AKT1-HA was detected by WB. Overexpression of Flag-CYPA or AKT1-HA alone was used as a negative control for the pulldown. **D** Exogenous CYPA interacts with AKT1 in HK-1 cells. Flag-CYPA and AKT1-HA plasmids were transiently transfected into the cells (4 μg/well of each plasmid in 100 mm dish). At 48 h post-transfection, the cells were collected and subjected to co-IP. Anti-HA (AKT1) antibody was used for pull-down. IgG was used as a negative control of pull-down. **E** Interaction of CYPA with AKT1 in 293 cells in the presence or absence of LMP1. The 293 cells were transiently transfected with LMP1-Flag and/or AKT1-HA plasmid (4 μg/well of each plasmid in 100 mm dish), respectively. At 48 h post-transfection, the cells were collected and subjected to co-IP. Endogenous CYPA was immune-precipitated by using anti-HA antibody for the pull-down, and was then detected by WB. Overexpression of LMP1-Flag or AKT1-HA alone was used as a negative control, respectively. **F** The effect of LMP1 on co-localization between CYPA and AKT1 by immunofluorescence staining. For LMP1 overexpression, the LMP1-Flag plasmid (2 μg/well in 6-well plate) was transfected into 293T cells, the cells were used for IF assay at 36 h post-transfection. The 293T cells without LMP1 overexpression was used for the contrast (upper). Scale bar, 20 μm.

maintenance of EBV genome that driven by the EBNA1 recruitment into the nucleus (Xin et al., 2019). Since CYPA is mostly expressed in cytoplasm, the potential mechanism that it is possibly involved in other signaling pathway spurred our interest. Therefore, in the present study, we further explored the function and mechanism of CYPA in the tumorigenicity of EBV-associated NPC.

As the result showed, the EBV oncoprotein LMP1 increased CYPA expression via NF-κB activation (Fig. 1). We examined that it could

promote cell proliferation and inhibit apoptosis, indicating its potential role in EBV-associated NPC. The results also demonstrated that EBV stimulated and hijacked host factors for its own need in oncogenesis as what we have showed elsewhere (Dang et al., 2021; Xin et al., 2019).

Aberrant AKT1 expression occurs frequently in various pathological conditions, such as cancers, inflammatory and autoimmune disorders (Manning and Toker, 2017). Evidences have shown that several proteins,
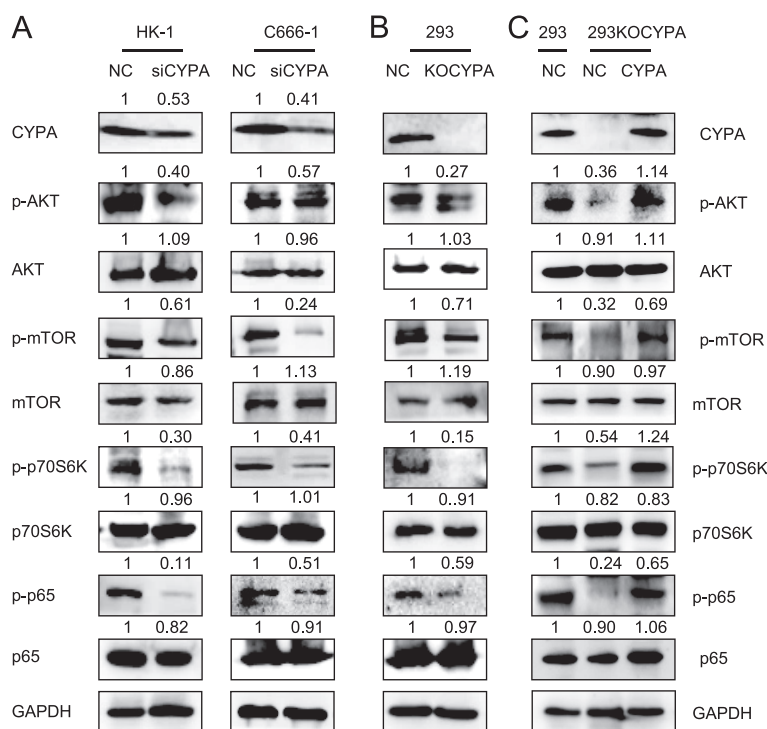
Fig. 5. The effect of CYPA on the activation of the AKT/mTOR and NF-κB signalings. **A** Effect of knockdown by siRNA-CYPA on the protein expressions of key molecules related to AKT/mTOR and NF-κB pathways in NPC cells. The siRNA (50 nmol/L per well in 6-well plate) was transfected into HK-1 and C666-1 cells respectively. At 48 h post-transfection, the cells were collected and subjected to Western blot (WB) assay. **B** Effect of CYPA knockout on the activation of AKT/mTOR and NF-κB pathways by WB assay. **C** Effect of CYPA overexpression on the restoration of the signalings regulated by CYPA knockout. The cells were transfected with Flag-CYPA plasmid (2 μg/well). At 48 h post-transfection, the cells were collected and subjected to WB. The 293 KOCYPA cell line was used in (**B**) and (**C**).

such as PI3K and PTEN, regulate the excessive activation of AKT (Gutierrez and Look, 2007). AKT1 is an essential serine/threonine kinase, and mainly serves as an effector kinase that plays roles at downstream of the PI3K (Manning and Toker, 2017). Phosphorylated AKT1 migrates to the cellular membrane and induces downstream signaling (Strickland and Vande Pol, 2016; Toker and Dibble, 2018; Yin et al., 2018). In the present approach, we provided evidence that CYPA bound to AKT1 to activate AKT/mTOR pathway in NPC, in which CYPA is upregulated by EBV-LMP1. Therefore, CYPA is a novel noncanonical AKT activator that is utilized by EBV-LMP1 to serve as an oncogene in NPC. AKT/mTOR is involved in multiple aspects of tumorigenesis, including cell growth, apoptosis, invasion, metastasis, and angiogenesis (Carnero et al., 2008; Shih et al., 2017). In addition, NF-κB can be activated by AKT/mTOR signaling in our study that is consistent with what was reported (Dan et al., 2008). Here, we revealed that CYPA was a key factor required for the activation of the AKT/mTOR/NF-κB signaling cascade. The results exhibited a mechanism to explain the previous observations why the master pathways of NF-κB, AKT, and mTOR are respectively associated with EBV infection in NPC (Bruce et al., 2021; Qin et al., 2017). More-over, the formation of CYPA-mediated NF-κB/AKT/mTOR/NF-κB posi-tive feedback loop assures the persistent activation of these pathways (Fig. 7). An oncogenic positive feedback loop is usually found to be important in cancer progression, which means the persistent activation of the loop without the sustained existence of the molecules triggering the loop at upstream. Therefore, the result suggests that LMP1 is not required to be constantly expressed for the continuous NF-κB and AKT/mTOR activation after the initial infection of EBV. The finding may partly explain that EBV is able to serve as a tumor-promoting factor but usually at a low level or even absent of expression in EBV-positive tumor tissues or cells (Cheung et al., 1999). This mechanism may also help EBV evade host surveillance during latent infection. Nevertheless, targeting one of the key factors in the feedback loop may subvert the efficiency of the viral
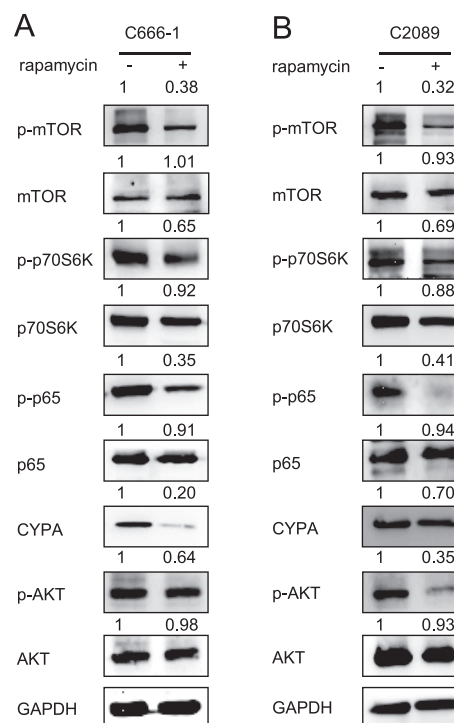

Fig. 6. The effect of rapamycin on the activation of CYPA/AKT/mTOR/NF-κB signaling cascade. **A, B** The key molecules of the CYPA/AKT/mTOR/NF-κB signaling cascade were detected by WB assays. EBV-positive C666-1 (**A**) and C2089 (**B**) cells were treated with the mTOR inhibitor, rapamycin (20 μmol/L), respectively. At 48 h post-treatment, the cells were collected and subjected to the detection.
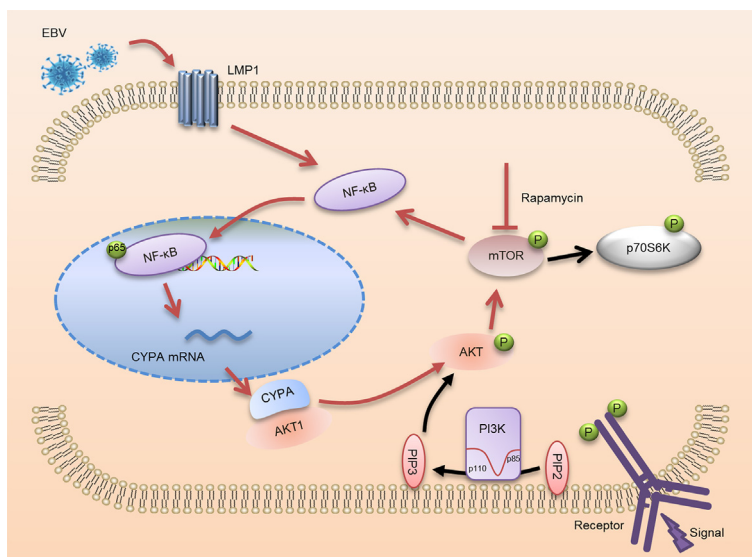
Fig. 7. Schematic of the mechanism on the activation of AKT/mTOR/NF-κB signaling cascade mediated by EBV-LMP1 upregulated CYPA.

tumorigenicity. Here we demonstrated that the mTOR inhibitor, rapamycin, restrained the activation of NF-κB/CYPA/AKT/mTOR/NF-κB positive feedback loop (Fig. 6).

5. Conclusions

In conclusion, CYPA is upregulated by EBV-LMP1 through NF-κB activation to serve as an oncogene in NPC cells. Mechanistically, CYPA is a novel AKT1 partner, thus activating AKT/mTOR and NF-κB pathways. Therefore, EBV induces the persistent potentiation of this signaling cascades through a positive feedback loop of NF-κB/CYPA/AKT/mTOR (Fig. 7). This study deepens the understanding on the causative role of EBV in tumorigenesis. The results also add to knowledge of the viral evasion from host surveillance during latent infection, providing potential therapeutic targets for EBV-associated NPC.

Data availability

All the data generated during the current study are included in the manuscript.

Ethics statement

No human subjects were used in this study. Animal experiments were approved by the IRB of Central South University.

Author contributions

Jianhong Lu: conceptualization, funding acquisition, supervision, writing - review & editing. Shuyu Xin: conceptualization, data curation, formal analysis, methodology, visualization, writing - original draft. Lingzhi Liu: conceptualization, formal analysis, writing - original draft. Yanling Li: data curation, software, validation. Jing Yang: data curation, software, validation. Shen Li: data curation, software, validation. Li Yang: data curation, software, validation. Taimei Cui: data curation, software, validation. Lielian Zuo: formal analysis, validation. Pengfei Cao and Qijia Yan: methodology, data curation.

Conflict of interest

The authors declare that there are no conflicts of interest in this work.

Appendix A. Supplementary data

Supplementary data to this article can be found online at https://doi.org/10.1016/j.virs.2022.09.001.

References

Baek, S.H., Ko, J.H., Lee, J.H., Kim, C., Lee, H., Nam, D., Lee, J., Lee, S.G., Yang, W.M., Um, J.Y., Sethi, G., Ahn, K.S., 2017. Ginkgolic acid inhibits invasion and migration and TGF-beta-induced EMT of lung cancer cells through PI3K/Akt/mTOR inactivation. J. Cell. Physiol. 232, 346–354.

Bahrami, B.F., Ataie-Kachoie, P., Pourgholami, M.H., Morris, D.L., 2014. p70 Ribosomal protein S6 kinase (Rps6kb1): an update. J. Clin. Pathol. 67, 1019–1025.

Bentz, G.L., Shackelford, J., Pagano, J., 2012. Epstein-Barr virus latent membrane protein 1 regulates the function of interferon regulatory factor 7 by inducing its sumoylation. J. Virol. 86, 12251–12261.

Bruce, J.P., To, K.F., Lui, V.W.Y., Chung, G.T.Y., Chan, Y.Y., Tsang, C.M., Yip, K.Y., Ma, B.B.Y., Woo, J.K.S., Hui, E.P., Mak, M.K.F., Lee, S.D., Chow, C., Velapasamy, S., Or, Y.Y.Y., Siu, P.K., El Ghamrasni, S., Prokopec, S., Wu, M., Kwan, J.S.H., Liu, Y., Chan, J.Y.K., van Hasselt, C.A., Young, L.S., Dawson, C.W., Paterson, I.C., Yap, L.F., Tsao, S.W., Liu, F.F., Chan, A.T.C., Pugh, T.J., Lo, K.W., 2021. Whole-genome profiling of nasopharyngeal carcinoma reveals viral-host co-operation in inflammatory NF-kappaB activation and immune escape. Nat. Commun. 12, 4193.

Bruce, J.P., Yip, K., Bratman, S.V., Ito, E., Liu, F.F., 2015. Nasopharyngeal cancer: molecular landscape. J. Clin. Oncol. 33, 3346–3355.

Carnero, A., Blanco-Aparicio, C., Renner, O., Link, W., Leal, J.F., 2008. The PTEN/PI3K/AKT signalling pathway in cancer, therapeutic implications. Curr. Cancer Drug Targets 8, 187–198.

Cheung, S.T., Huang, D.P., Hui, A.B., Lo, K.W., Ko, C.W., Tsang, Y.S., Wong, N., Whitney, B.M., Lee, J.C., 1999. Nasopharyngeal carcinoma cell line (C666-1) consistently harbouring Epstein-Barr virus. Int. J. Cancer 83, 121–126.

Chu, M.Y., Huang, H.C., Li, E.M., Xu, L.Y., 2021. CypA: a potential target of tumor radiotherapy and/or chemotherapy. Curr. Med. Chem. 28, 3787–3802.

Chung, G.T., Lou, W.P., Chow, C., To, K.F., Choy, K.W., Leung, A.W., Tong, C.Y., Yuen, J.W., Ko, C.W., Yip, T.T., Busson, P., Lo, K.W., 2013. Constitutive activation of distinct NF-kappaB signals in EBV-associated nasopharyngeal carcinoma. J. Pathol. 231, 311–322.

Dan, H.C., Cooper, M.J., Cogswell, P.C., Duncan, J.A., Ting, J.P., Baldwin, A.S., 2008. Akt-dependent regulation of NF-{kappa}B is controlled by mTOR and Raptor in association with IKK. Genes Dev. 22, 1490–1500.

Dang, W., Cao, P., Yan, Q., Yang, L., Wang, Y., Yang, J., Xin, S., Zhang, J., Li, J., Long, S., Zhang, W., Zhang, S., Lu, J., 2021. IGFBP7-AS1 is a p53-responsive long noncoding RNA downregulated by Epstein-Barr virus that contributes to viral tumorigenesis. Cancer Lett. 523, 135–147.

Davra, V., Saleh, T., Geng, K., Kimani, S., Mehta, D., Kasikara, C., Smith, B., Colangelo, N.W., Ciccarelli, B., Li, H., Azzam, E.I., Kalodimos, C.G., Birge, R.B., Kumar, S., 2020. Cyclophilin A inhibitor debio-025 targets crk, reduces metastasis, and induces tumor immunogenicity in breast cancer. Mol. Cancer Res. 18, 1189–1201.

Dawar, F.U., Tu, J., Khattak, M.N., Mei, J., Lin, L., 2017. Cyclophilin A: a key factor in virus replication and potential target for anti-viral therapy. Curr. Issues Mol. Biol. 21, 1–20.

Delecluse, H.J., Hilsendegen, T., Pich, D., Zeidler, R., Hammerschmidt, W., 1998. Propagation and recovery of intact, infectious Epstein-Barr virus from prokaryotic to human cells. Proc. Natl. Acad. Sci. U. S. A. 95, 8245–8250.

Gandhi, M.K., Tellam, J.T., Khanna, R., 2004. Epstein-Barr virus-associated Hodgkin's lymphoma. Br. J. Haematol. 125, 267–281.

Guo, M., James, A.W., Kwak, J.H., Shen, J., Yokoyama, K.K., Ting, K., Soo, C.B., Chiu, R.H., 2016. Cyclophilin A (CypA) plays dual roles in regulation of bone anabolism and resorption. Sci. Rep. 6, 22378.

Gutierrez, A., Look, A.T., 2007. NOTCH and PI3K-AKT pathways intertwined. Cancer Cell 12, 411–413.

Huang, S.C.M., Tsao, S.W., Tsang, C.M., 2018. Interplay of viral infection, host cell factors and tumor microenvironment in the pathogenesis of nasopharyngeal carcinoma. Cancers 10, 106.

Kang, M.S., Kieff, E., 2015. Epstein-Barr virus latent genes. Exp. Mol. Med. 47, e131.

Kim, S.W., Kim, S.M., Bae, H., Nam, D., Lee, J.H., Lee, S.G., Shim, B.S., Kim, S.H., Ahn, K.S., Choi, S.H., Sethi, G., Ahn, K.S., 2013. Embelin inhibits growth and induces apoptosis through the suppression of Akt/mTOR/S6K1 signaling cascades. Prostate 73, 296–305.

Lin, D.C., Meng, X., Hazawa, M., Nagata, Y., Varela, A.M., Xu, L., Sato, Y., Liu, L.Z., Ding, L.W., Sharma, A., Goh, B.C., Lee, S.C., Petersson, B.F., Yu, F.G., Macary, P., Oo, M.Z., Ha, C.S., Yang, H., Ogawa, S., Loh, K.S., Koeffler, H.P., 2014. The genomic landscape of nasopharyngeal carcinoma. Nat. Genet. 46, 866–871.

Liu, L., Zhou, Q., Xie, Y., Zuo, L., Zhu, F., Lu, J., 2017. Extracellular vesicles: novel vehicles in herpesvirus infection. Virol. Sin. 32, 349–356.

Liu, L., Zuo, L., Yang, J., Xin, S., Zhang, J., Zhou, J., Li, G., Tang, J., Lu, J., 2019a. Exosomal cyclophilin A as a novel noninvasive biomarker for Epstein-Barr virus associated nasopharyngeal carcinoma. Cancer Med. 8, 3142–3151.

Liu, R., Qu, Z., Lin, Y., Lee, C.S., Tai, W.C., Chen, S., 2019b. Brevilin A induces cell cycle arrest and apoptosis in nasopharyngeal carcinoma. Front. Pharmacol. 10, 594.

Lo, K.W., Chung, G.T., To, K.F., 2012. Deciphering the molecular genetic basis of NPC through molecular, cytogenetic, and epigenetic approaches. Semin. Cancer Biol. 22, 79–86.

Lu, J., Han, Z., Liu, Y., Liu, W., Lee, M.S., Olson, M.A., Ruthel, G., Freedman, B.D., Harty, R.N., 2014. A host-oriented inhibitor of Junin Argentine hemorrhagic fever virus egress. J. Virol. 88, 4736–4743.

Lu, J., Qu, Y., Liu, Y., Jambusaria, R., Han, Z., Ruthel, G., Freedman, B.D., Harty, R.N., 2013. Host IQGAP1 and Ebola virus VP40 interactions facilitate virus-like particle egress. J. Virol. 87, 7777–7780.

Lu, J.H., Tang, Y.L., Yu, H.B., Zhou, J.H., Fu, C.Y., Zeng, X., Yu, Z.Y., Yin, H.L., Wu, M.H., Zhang, J.Y., Li, X.L., Li, G., 2010. Epstein-Barr virus facilitates the malignant potential of immortalized epithelial cells: from latent genome to viral production and maintenance. Lab. Invest. 90, 196–209.

Manning, B.D., Cantley, L.C., 2007. AKT/PKB signaling: navigating downstream. Cell 129, 1261–1274.

Manning, B.D., Toker, A., 2017. AKT/PKB signaling: navigating the network. Cell 169, 381–405.

Mohan, C.D., Srinivasa, V., Rangappa, S., Mervin, L., Mohan, S., Paricharak, S., Baday, S., Li, F., Shanmugam, M.K., Chinnathambi, A., Zayed, M.E., Alharbi, S.A., Bender, A., Sethi, G., Basappa, Rangappa, K.S., 2016. Trisubstituted-imidazoles induce apoptosis in human breast cancer cells by targeting the oncogenic PI3K/Akt/mTOR signaling pathway. PLoS One 11, e0153155.

Nakanishi, Y., Wakisaka, N., Kondo, S., Endo, K., Sugimoto, H., Hatano, M., Ueno, T., Ishikawa, K., Yoshizaki, T., 2017. Progression of understanding for the role of Epstein-Barr virus and management of nasopharyngeal carcinoma. Cancer Metastasis Rev. 36, 435–447.

Nigro, P., Pompilio, G., Capogrossi, M.C., 2013. Cyclophilin A: a key player for human disease. Cell Death Dis. 4, e888.

Nishikawa, J., Iizasa, H., Yoshiyama, H., Shimokuri, K., Kobayashi, Y., Sasaki, S., Nakamura, M., Yanai, H., Sakai, K., Suehiro, Y., Yamasaki, T., Sakaida, I., 2018. Clinical importance of Epstein(-)Barr virus-associated gastric cancer. Cancers (Basel) 10, 167.

Polivka Jr., J., Janku, F., 2014. Molecular targets for cancer therapy in the PI3K/AKT/mTOR pathway. Pharmacol. Ther. 142, 164–175.

Qin, L., Li, X., Lin, Z., Li, H., Mo, Y., Su, F., Mo, W., Yang, Z., 2017. EBV-LMP1 regulating AKT/mTOR signaling pathway and WWOX in nasopharyngeal carcinoma. Int. J. Clin. Exp. Pathol. 10, 8619–8625.

Shair, K.H.Y., Reddy, A., Cooper, V.S., 2018. New insights from elucidating the role of LMP1 in nasopharyngeal carcinoma. Cancers (Basel) 10, 86.

Shih, Y.L., Chou, H.M., Chou, H.C., Lu, H.F., Chu, Y.L., Shang, H.S., Chung, J.G., 2017. Casticin impairs cell migration and invasion of mouse melanoma B16F10 cells via PI3K/AKT and NF-kappaB signaling pathways. Environ. Toxicol. 32, 2097–2112.

Siveen, K.S., Ahn, K.S., Ong, T.H., Shanmugam, M.K., Li, F., Yap, W.N., Kumar, A.P., Fong, C.W., Tergaonkar, V., Hui, K.M., Sethi, G., 2014. Y-tocotrienol inhibits angiogenesis-dependent growth of human hepatocellular carcinoma through abrogation of AKT/mTOR pathway in an orthotopic mouse model. Oncotarget 5, 1897–1911.

Strickland, S.W., Vande Pol, S., 2016. The human papillomavirus 16 E7 oncoprotein attenuates AKT signaling to promote internal ribosome entry site-dependent translation and expression of c-MYC. J. Virol. 90, 5611–5621.

Takada, H., Imadome, K.I., Shibayama, H., Yoshimori, M., Wang, L., Saitoh, Y., Uota, S., Yamaoka, S., Koyama, T., Shimizu, N., Yamamoto, K., Fujiwara, S., Miura, O., Arai, A., 2017. EBV induces persistent NF-kappaB activation and contributes to survival of EBV-positive neoplastic T- or NK-cells. PLoS One 12, e0174136.

Toker, A., Dibble, C.C., 2018. PI 3-kinase signaling: AKTing up inside the cell. Mol. Cell 71, 875–876.

Tu, C., Zeng, Z., Qi, P., Li, X., Guo, C., Xiong, F., Xiang, B., Zhou, M., Liao, Q., Yu, J., Li, Y., Li, X., Li, G., Xiong, W., 2018. Identification of genomic alterations in nasopharyngeal carcinoma and nasopharyngeal carcinoma-derived Epstein-Barr virus by whole-genome sequencing. Carcinogenesis 39, 1517–1528.

Wang, G., Shen, J., Sun, J., Jiang, Z., Fan, J., Wang, H., Yu, S., Long, Y., Liu, Y., Bao, H., Zhang, K.X., Han, K., Zhu, M., Zheng, Y., Lin, Z., Jiang, C., Guo, M., 2017. Cyclophilin A maintains glioma-initiating cell stemness by regulating wnt/beta-catenin signaling. Clin. Cancer Res. 23, 6640–6649.

West, R.B., 2014. Fingerprints of Epstein-Barr virus in nasopharyngeal carcinoma. Nat. Genet. 46, 809–810.

Wu, C.C., Fang, C.Y., Huang, S.Y., Chiu, S.H., Lee, C.H., Chen, J.Y., 2018. Perspective: contribution of epstein-barr virus (EBV) reactivation to the carcinogenicity of nasopharyngeal cancer cells. Cancers (Basel) 10, 120.

Xin, S., Du, S., Liu, L., Xie, Y., Zuo, L., Yang, J., Hu, J., Yue, W., Zhang, J., Cao, P., Zhu, F., Lu, J., 2019. Epstein-barr virus nuclear antigen 1 recruits cyclophilin A to facilitate the replication of viral DNA genome. Front. Microbiol. 10, 2879.

Yamamoto, T., Takakura, H., Mitamura, K., Taga, A., 2020. Cyclophilin a knockdown inhibits cell migration and invasion through the suppression of epithelial-mesenchymal transition in colorectal cancer cells. Biochem. Biophys. Res. Commun. 526, 55–61.

Yang, J., Zhou, M., Zhao, R., Peng, S., Luo, Z., Li, X., Cao, L., Tang, K., Ma, J., Xiong, W., Fan, S., Schmitt, D.C., Tan, M., Li, X., Li, G., 2014. Identification of candidate biomarkers for the early detection of nasopharyngeal carcinoma by quantitative proteomic analysis. J. Proteomics 109, 162–175.

Yi, M., Cai, J., Li, J., Chen, S., Zeng, Z., Peng, Q., Ban, Y., Zhou, Y., Li, X., Xiong, W., Li, G., Xiang, B., 2018. Rediscovery of NF-kappaB signaling in nasopharyngeal carcinoma: how genetic defects of NF-kappaB pathway interplay with EBV in driving oncogenesis? J. Cell. Physiol. 233, 5537–5549.

Yin, Y., Dang, W., Zhou, X., Xu, L., Wang, W., Cao, W., Chen, S., Su, J., Cai, X., Xiao, S., Peppelenbosch, M.P., Pan, Q., 2018. PI3K-Akt-mTOR axis sustains rotavirus infection via the 4E-BP1 mediated autophagy pathway and represents an antiviral target. Virulence 9, 83–98.

Yu, J.S., Cui, W., 2016. Proliferation, survival and metabolism: the role of PI3K/AKT/mTOR signalling in pluripotency and cell fate determination. Development 143, 3050–3060.

Yuan, Y., Hou, X., Feng, H., Liu, R., Xu, H., Gong, W., Deng, J., Sun, C., Gao, Y., Peng, J., Wu, Y., Li, J., Fang, C., Chen, Q., 2016. Proteomic identification of cyclophilin A as a potential biomarker and therapeutic target in oral submucous fibrosis. Oncotarget 7, 60348–60365.

Zhu, D., Wang, Z., Zhao, J.J., Calimeri, T., Meng, J., Hideshima, T., Fulciniti, M., Kang, Y., Ficarro, S.B., Tai, Y.T., Hunter, Z., McMilin, D., Tong, H., Mitsiades, C.S., Wu, C.J., Treon, S.P., Dorfman, D.M., Pinkus, G., Munshi, N.C., Tassone, P., Marto, J.A., Anderson, K.C., Carrasco, R.D., 2015. The Cyclophilin A-CD147 complex promotes the proliferation and homing of multiple myeloma cells. Nat. Med. 21, 572–580.

Zuo, L., Xie, Y., Tang, J., Xin, S., Liu, L., Zhang, S., Yan, Q., Zhu, F., Lu, J., 2019. Targeting exosomal EBV-LMP1 transfer and miR-203 expression via the NF-kappaB pathway: the therapeutic role of aspirin in NPC. Mol. Ther. Nucleic Acids 17, 175–184.

Zuo, L., Yu, H., Liu, L., Tang, Y., Wu, H., Yang, J., Zhu, M., Du, S., Zhao, L., Cao, L., Li, G., Lu, J., 2015. The copy number of Epstein-Barr virus latent genome correlates with the oncogenicity by the activation level of LMP1 and NF-kappaB. Oncotarget 6, 41033–41044.